Published in final edited form as:
Lasers Surg Med. 2008 October ; 40(8): 562–569. doi:10.1002/lsm.20663.

Viability of Human Septal Cartilage After 1.45 μm Diode Laser Irradiation

Ick-Soo Choi, MD[1,*], **Yong-Seok Chae, PhD**[2], **Allison Zemek**[2], **Dmitry E. Protsenko, PhD**[2], and **Brian Wong, MD, PhD**[2,3,4]

[1]Department of Otolaryngology, Head and Neck Surgery, Seoul Paik Hospital, Inje University, 5 Mareunnae Gil, Jung Gu, Seoul 100032, Korea

[2]Beckman Laser Institute and Medical Clinic, University of California Irvine, 1002 Health Sciences Road East, Irvine, California 92612

[3]Department of Otolaryngology, Head and Neck Surgery, University of California Irvine, 101 The City Drive, Orange, California 92668

[4]Department of Biomedical Engineering, Samueli School of Engineering, University of California Irvine, Irvine, California 92697

Abstract

Background and Objectives—Chondrocyte viability following laser irradiation and reshaping has not been established for human nasal septal cartilage. Knowledge of the relationship between thermal injury and laser dosimetry is needed in order to optimize septal laser cartilage reshaping. The objective of this study was to determine the depth and width of thermal injury in human septal cartilage following laser irradiation.

Study Design/Materials and Methods—Excess fresh nasal septal cartilage sections from rhinoplasty or septoplasty operations were irradiated using a 1.45 μm diode laser 1.25–3.6 W (2.8 mm spot diameter) with 1 second fixed exposure time, and then at exposure times of 1–4 seconds for a fixed power of 1.25 W. An infrared camera recorded surface temperature profiles during irradiation, and the temperature data were incorporated into a rate process model to numerically estimate thermal damage. Calcein AM and ethidium homodimer-1 fluorescent dyes combined with confocal laser microscopy (CLM) were used to measure thermal damage.

Results—CLM demonstrated clear demarcation between dead and living cells following irradiation. The extent of non-viable chondrocyte distributions increased with power and exposure time. The maximum depths of injury were 1,012 and 1,372 μm after 3.6 W 1 second and 1.25 W 4 seconds irradiation respectively. The damage predictions made by the rate process model underestimated thermal injury when compared with CLM measurements.

Conclusions—The assay system identified regions of non-viable chondrocytes in human septal cartilage and defined how thermal injury varies with dosimetry when using a 1.45 μm diode laser.

[*]Correspondence to: Ick-Soo Choi, MD, Department of Otolaryngology, Head and Neck Surgery, Seoul Paik Hospital, Inje University, 5 Mareunnae Gil, Jung Gu, Seoul 100032, Korea, cisoo99@yahoo.co.kr.

Keywords

laser; cartilage reshaping; confocal; chondrocyte viability; rate process models; thermal damage; infrared thermography; human; septoplasty; nose; rhinoplasty

Introduction

The sustained plastic deformation of cartilage following laser irradiation, also known as laser cartilage reshaping (LCR), was originally introduced in 1993 [1]. Several studies have reported successful clinical application of non-ablative laser facial cartilage reshaping during septoplasty [2,3] and otoplasty operations [4]. Notably septal cartilage reshaping using transmucosal laser irradiation has been evaluated in a large numbers of patients and found to be reasonably efficient and safe [3]. The technique is incisionless and uses topical anesthesia, and when performed correctly may avoid the potential complications of conventional septoplasty by maintaining mucoperichondrial integrity. However, outside of specialized academic centers, the technique has not been widely adopted for several reasons, most of which center upon surgeons' concerns over thermal damage produced by laser irradiation. The underlying mechanisms responsible for accelerated stress relaxation during LCR are not completely understood, but are thought to rely upon a number of processes including the mass transfer of water and matrix protein denaturation [2]. Regardless of the precise mechanism of action, a major concern with LCR focuses on the potential thermal injury to the chondrocytes during photothermal heating. While temperature dependent thermal injury has been studied using many different laser and other heating systems in ex vivo animal cartilages [5–9], no studies have systematically evaluated the effects of laser dosimetry on human nasal septal cartilage. This information is critically important, especially if LCR is to gain broader clinical acceptance. Many techniques can be used to assess chondrocyte viability [10,11], however gauging acute thermal injury may be best accomplished using a Live/Dead viability assay system combined with laser confocal microscopy [12–15]. Recent studies on laser mediated shape change and resultant tissue viability using the Live/Dead assay approach demonstrated that significant thermal damage is concurrent with clinically relevant shape change on animal septal cartilage [7–9]. These studies are at variance with previous hypothesis that there is a privileged laser dosimetry parameter where clinically relevant shape change and tissue viability coexist. Therefore understanding the extent of thermal injury produced by lasers used in the reshaping of human septal cartilage is extremely important.

The selection of appropriate laser wavelengths to perform reshaping is an important issue and is a major factor in determining the temporal and spatial evolution of heat during LCR. Initially for practical purposes, the CO_2 laser (λ=10.6 μm) was used when LCR was introduced [1], followed shortly thereafter by applications using deeper penetrating lasers such as Ho:YAG (λ=2.1 μm) [2] and Nd:YAG (λ=1.32 μm).It became readily apparent that the high absorption of CO_2 and Ho:YAG laser radiation in water results in penetration depth too shallow for efficient volumetric heating of human septum while low absorption and corresponding high penetration of the Nd:YAG laser radiation might result in septum perforation. Hence laser wavelength selection has focused on those devices centered around

the relative absorption peak of water at about 1.45 μm. Recent studies have focused on the use of 1,540 nm Er:Glass fiber lasers and semiconductor laser devices emitting at 1,450 and 1,540 nm [16,17]. These specific infrared laser wavelengths have optical penetration depths that are on the scale of the nasal septum thickness. The purpose of this study is to determine the axial (depth) extent of thermal injury produced by 1.45 mm diode laser using a Live/Dead viability assay system.

Materials and Methods

Excess septal cartilage from 17 patients undergoing either septoplasty or septorhinoplasty was obtained in accord with the guidelines established by the Institutional Review Board at the University of California Irvine. The specimens were stored in saline solution at 48°C for no longer than 24 hours following surgery before laser irradiation. Prior to use, specimens were equilibrated in a room temperature saline bath for at least 15 minutes. Specimens were approximately 1–2 mm thick and roughly rectangular, though shape varied widely as these were surgical remnants.

Laser Irradiation

Light from a diode laser (1.45 μm, Candela, Wayland, MA) was delivered via a 1.5 mm diameter silica fiber and aimed at the tissue. Laser power was measured using an optical power meter (Newport Corp., Irvine, CA). The diode laser system was controlled using software written in LabVIEW (National Instruments, Austin, TX) running on a computer workstation. Specimens were segregated into two groups differing with either fixed exposure time or power. For a fixed exposure time group (1 second), specimens were irradiated at 1.25, 1.68, 2.15, 2.7, 3.2, and 3.6 W (2.8 mm spot diameter). For a fixed laser power 1.25 W, exposure times of 1, 2, 3, and 4 seconds were used. These setting were selected on the basis of preliminary studies which narrowed the laser dosimetry parameters and identified potential values of interest. Irradiation was performed with the specimens suspended on top of an array of taxidermy pinpoints. Suspension on taxidermy pins minimizes contact with conductive materials that could potentially serve as secondary heat sources or sinks. Light from the laser was directed perpendicularly at the specimen and the distance from the fiber tip to tissue surface was 3 mm.

Cell Viability Assay

Within 2 hours after laser irradiation, a 400 μm wide cross-section through the center of the laser target site was excised for use in viability staining. The assay was performed with calcein AM and ethidium homodimer-1 (EthD-1) (Molecular Probes, Eugene, OR) combined with laser confocal microscopy (Zeiss, Göttingen, Germany). The specimens were soaked in 1.0 ml of Hank's Buffered Saline Solution (HBSS) containing 0.6 μl calcein AM and 13 μl EthD-1 for 30 minutes in darkness. Stained cross-sectional slices of specimens were inspected with the laser-scanning confocal microscope employing a 488 nm argon laser excitation source at 10× magnification. Calcein AM when used as a “live” stain is indicator of cells which have intact cell membranes and esterase activity. It is a fluorogenic esterase substrate hydrolyzed by living cells to yield a green fluorescent product. The second stain, EthD-1, can only permeate cells with compromised membranes, which weakly binds

to DNA while binding to RNA with high affinity. Therefore, cell death, or EthD-1 staining, is determined based on membrane integrity. The differential fluorescent signals from these two dyes were collected independently via two separate color channels. While the images were stored as a combination of both red and green channels, these channels can also be viewed independently. All images were saved on the computer system linked with the confocal microscope, and subsequently transferred via portable media to another computer for analysis.

Images of stained specimens were analyzed using Photoshop (version 9.0, Adobe Systems, Inc., San Jose, CA). At 10× magnification, the field of view of the microscope is 1,278 μm×1,278 μm. Montages that encompass two cross-sections were assembled. The depth and width of "dead" region was determined by inspection of image in the green channel. Geometrical data from five specimens were averaged.

Temperature Measurements

The surface temperature of the cartilage samples before, during, and after irradiation were recorded with a single element HgCd infrared thermal imaging system and attached 3× magnifying lens (Inframetrics, Model 600, S/N 7459, Billerica, MA). The system generates images by raster scanning the focal point across the object plane. Emissivity was set to 1. The specimen surface was at a focal distance of 122 mm away from the objective lens of the camera. The focal distance was determined by imaging an aluminum ruler with black inked markings and adjusting the camera position until the lettering was sharply in focus. The orientation of the cartilage sample was such that the laser beam was orthogonal to the surface of the specimen. The thermal camera was aligned to the cartilage sample at an angle slightly less than 90° so that the laser fiber assembly would not eclipse the laser spot on the specimen surface. The viewing axis of the camera is not completely normal to the surface of the cartilage and the thermal image is slightly distorted. However, the analysis of thermal image was performed in the area of interest, which spans the diameter of the laser spot perpendicular to both laser fiber and thermal camera axis, and were geometrical distortions are minimal [9]. The specimen was imaged for 3 to 5 seconds prior to irradiation, then for the duration of irradiation, and for 20–25 seconds after irradiation. At that point, the specimen surface temperature returned to approximately ambient temperature. The video output of the thermal imaging system was recorded on digital video (DV) with a camcorder (Optura 20, Canon U.S.A., Lake Success, NY). The DV data were then converted to an audio video interleave formatted file (".avi") using a video editing program (Pinnacle Studio 9.1, Pinnacle Systems, Inc., Mountain View, CA). The video files were subsequently trimmed to 30 seconds and compressed using Intel Indeo® Video R3.2 to preserve the 620×480 pixel array output from the thermal camera. The .avi files were then analyzed with a custom program written in Matlab 7 (The Mathworks, Natick, MA). The program converts the 620×480 grayscale pixel matrix for each frame into numerical values which correspond linearly to pixel intensity. Then, the center of the laser spot is determined with a small margin of error by inspection. The program then references the designated laser spot center and analyzes the 10 pixel wide band spanning the diameter of the laser spot on the cartilage specimen. The data from this 600×10 value matrix is then averaged to form a dimensional line plot for a given point in time, with the pixel number on the *x*-axis (corresponding to

spatial location along the spot diameter) and temperature on the *y*-axis. There is one line plot generated for every frame of the avi video clip. Then, using these line plots, the program tracks the temperature history at user-defined distances (or radii) from the center of the laser spot; for this study, the radii of interest were 0 to 4.5 mm in 0.5 mm increments (there are approximately 42.54 pixels per mm using the geometry of the current set-up). The information is compiled to produce multiple temperature history plots at each of the designated radii, with time as the abscissa (*x*-axis), and with temperature as the ordinate (*y*-axis). The thermal imaging system was calibrated using a blackbody source (BB701, OMEGA Engineering Ltd, Stamford, CT). The device was focused slightly past the surface of the blackbody. Temperatures were recorded for 5 seconds by the thermal camera for each blackbody temperature. The specified blackbody temperatures were plotted versus the temperatures measured by the thermal camera and a calibration curve was thus constructed. By maintaining the same range and offset settings on the thermal camera for all studies, a third-degree quadratic calibration equation was generated.

Rate Process Analysis

Thermal damage was estimated using a rate process model and the time-temperature data. We assumed that thermal damage to chondrocytes in cartilage can be described as a first-order thermal-chemical rate process, in which the time-dependent temperature history determines damage. Irreversible damage occurs as a single-step molecular transformation, where heat produces transformation of various intra-molecular bonds in matrix macromolecules and may result in cell death [18–27]. The rate process model and the derivation of the frequency factor, A, and activation energy, E_a, are described elsewhere and will only be briefly reviewed here [6,28]. Damage ($\Omega(\tau)$) can be estimated by integrating the Arrhenius damage integral [6]:

$$\Omega(\tau)=A\int_0^{\tau} e^{-\frac{E_a}{RT(t)}}dt \quad (1)$$

In this damage model, thermal injury is defined to occur when $\Omega(\tau)= 1$, or in other words where the remaining fraction of live cells is equal to 1/e of the initial cell population. In our prior work, we used the live-dead assay system to estimate the rate process coefficients and calculated E_a (4.5×10^5 J mol^{-1}) and A (1.2×10^{70} second^{-1}). The coefficients were determined in experiments based on precisely controlled heating of rabbit septal cartilage, and the quantitative analysis of tissue damage using flow cytometry and differential cell staining [6]. These values were later verified by comparing numerical estimates with the size of thermal injury zones created in rabbit septal cartilage using an Nd:YAG laser [9]. In this experiment, $\Omega(\tau)$ was calculated at a finite number of radial distances from the center of the laser spot. Since the thermal camera acquires data at 29.97 frames per second, there is adequate temporal resolution to numerically integrate the damage integral. As the calculations for $\Omega(\tau)$ are exquisitely sensitive to small changes in temperature, the radial distance which yielded the $\Omega(\tau)$ value closest to 1 was designated as the distance at which there is a transition between normal viable tissue and that which has undergone significant thermal injury.

Results

Frank ablation was not observed with any of the dosimetry parameters used in this study. The Live/Dead assay using confocal microscopy demonstrated a relatively sharp demarcation between live cells (green) and dead cells (red) in cross-section. The dosimetry pair of 1.25 W with 1 second irradiation was the minimal threshold at which any thermal injury could be identified using this system. All thermal lesions had a shape closely approximated by a spherical section with the maximum width measured at the irradiated surface of the specimen. As expected, the dimensions of this region of damaged tissue increased with both power and exposure time (Figs. 1 and 2). The average depth and width of the thermally damaged regions are listed in Tables 1 and 2 for a fixed irradiation time of 1 second (with variable laser power) and for a fixed laser power of 1.25 W (with variable irradiation time), respectively. The data in Table 1 shows that depth and width of thermal injury increased with power from 436 to 1,012 μm and from 1,336 to 2,666 μm, respectively. Likewise, as exposure time increased, the depth increased from 436 to 1,372 μm and width from 1,336 to 3,024 μm. When damage is plotted as a function of total energy delivery, we observe a near linear dependence for depth (Fig. 3). The width is not a linear function of the energy: its rate of increase is reduced with increase in energy (Fig. 4). The numerical estimates of thermal damage derived using the rate process model systematically underestimated thermal injury (Fig. 5).

Discussion

Identifying the optimal laser dosimetry pairs to perform septal LCR is critically important in order for this technology to gain broader clinical acceptance outside of academic centers. In LCR, mechanically deformed cartilage tissue is focally heated with a laser. The energy is directed toward regions of the specimen where internal stress is increased. The generation of heat within the tissue leads to reduction of this stress (mechanical relaxation), and establishment of a new equilibrium shape. Optimization of LCR requires: (1) knowing of the effect of photothermal heating on the mechanical properties of tissue, (2) understanding how tissue viability varies with laser dosimetry, and (3) identifying laser targets sites across the surface of a potentially complex structure. Our previous work with ex vivo cartilage tissue and in animal models have focused on these three areas, and has led to the current research directed at facilitating broader clinical use of this technology. The present work has focused on determining how human septal cartilage viability varies with dosimetry, using a laser wavelength that has been demonstrated to be effective in clinical septal cartilage reshaping. In LCR, there is a tradeoff between the shape change and thermal injury, and the two often go hand in hand. In previous work, we have demonstrated that with certain wavelengths and laser dosimetry, thermal injury and mechanical relaxation are not mutually exclusive, and the efficacy of LCR relies upon spatially selective heating rather than some privileged laser dosimetry parameter space where shape change and viability coexist. Given this assertion, it is critically important to both know and limit the extent of tissue injury during septal LCR, as a full-thickness septal injury would lead to a perforation. In septal LCR, the depth of laser heating must be adequate to produce mechanical relaxation in a region of interest large enough to lead to overall structural shape change, yet at the same time it must not produce a full-thickness injury to the cartilage. Confocal microscopy with the Live/Dead assay reveals

the extent of thermal injury in cartilage more accurately than conventional histology [15]. Generally, thermal injury in biological tissues depends on the combination of the temperature elevation and heating time or heating history as embodied in the Arrhenius integral above. The sharp demarcation (approximately one cell wide) between damaged and viable cell zones observed at all combinations of laser power and irradiation time (Figs. 1 and 2) is characteristic of damage zones created in the presence of very steep thermal gradient [28,29]. Temperature distribution within the laser irradiated specimen and, subsequently, extent of thermal injury is described by the heat diffusion equation:

$$k\nabla^2 T + q = \rho C_{\mathrm{p}} \frac{\partial T}{\partial t} \quad (2)$$

where k, ρ, and C_{p} are tissue thermal conductivity, density and heat capacity, respectively, and q is volumetric heat source (power density) created in tissue due to absorption of laser light [30]. In this equation the left-hand terms describe heat diffusion and heat generation and the right-hand term describes heat storage in tissue. In the absence of heat diffusion, temperature within cartilage specimen is proportional to the laser generated volumetric heat source, q:

$$T(\tau) = \int_0^{\tau} \frac{q}{\rho C_{\mathrm{p}}} \mathrm{d}t = \frac{q\tau}{\rho C_{\mathrm{p}}} \quad (3)$$

Increase in either laser power or irradiation time will increase delivered energy and proportionately increase tissue volume heated to or above thermal injury threshold, $\Omega = 1$. Figure 3 demonstrates near linear dependence of thermal injury depth and the delivered laser energy suggesting that within the sample heat is not efficiently removed from the volume absorbing laser light (so-called thermal confinement) [31]. This localized heating and concomitant linear increase in thermal injury dimension with energy greatly simplifies the task of a priori determining the depth of tissue injury: injury depth simply scales linearly with power and irradiation time. In contrast, the width of the thermal zone does not scale linearly with delivered energy (Fig. 4) indicating that heat transfer makes a significant contribution. In all experiments, damage zones were the widest at the surface of the sample where removal of heat by diffusion into surrounding tissue is accompanied by convection into air. However, in case of transmucosal irradiation of the septum as used in clinical practice, convective heat removal will occur at the mucosal surface and it is likely that beneath it in all heated volume of cartilage heat will be dissipated by conduction only. Therefore, it is likely that width of thermal injury in septal cartilage covered by mucosa will scale linearly with laser dosimetry. It should be noted that during transmucosal irradiation of the septum a portion of laser energy will be absorbed by the mucosa and the dimensions of thermal injury zone in the septal cartilage may actually be smaller for a given dosimetry. Regardless, the resulting damage size increases predictably with both power and laser exposure time.

The rate process model (Eq. 1) is sensitive to values of the model coefficients, A and E_{a} [25,28]. To date, the thermal damage coefficients for human septal cartilage have not been

measured. The present numerical estimates used the thermal damage coefficients for cartilage obtained from our previous rabbit tissue studies. Subtle differences between human and rabbit cartilage may account for why the model systematically underestimates the damage dimensions in the present application.

Generally the laser irradiation of amorphous tissue like cartilage results in highly reproducible tissue responses. The observed variability in the measured damage size may result from irregular surface features, micro-cracks, or small defects that occurred during septal surgery or may be simply due to regional variations as these surgical remnants were obtained from different locations within the septum. Another source of the variation in the data is technical limitations obtaining a cross-section through the exact center of the laser spot for confocal imaging.

There is a controversy about chondrocyte viability following LCR and laser irradiation [5,7–9,30]. Sviridov suggested that specific laser dosimetry parameters may exist that would facilitate cartilage shape change without causing permanent damage to chondrocytes. They used conventional light microscopy to qualitatively identify features of thermal injury in chondrocytes which included: (1) focal cytoplasmic vacuolation which they believe is associated with reversible cell injury and; (2) nuclear condensation which is indicative of cell death [5]. Mainil-Varlet et al. [15] used both conventional histology and “Live/Dead assays” with confocal microscopy in their study of laser effects on articular cartilage thermal damage in Ho:YAG laser irradiated cartilage tissue using Alcian blue and safranin O-fast green staining in combination with light microscopy; zone 1: vacuolation with loss of cell structure, disappearance of nuclei and other organelles; zone 2: small damaged cells containing condensed or marginalized nuclei; and zone 3: proteoglycan depletion without major cell alteration. The more intriguing elements of their work compared histology and confocal imaging. The Live/Dead viability assay identified a zone of thermal damage that exceeded three times the damage seen using light microscopy. At least according to this result, both histologic regions identified in Sviridov's work would likely reside in this region of devitalized tissue using confocal imaging. The “Live/Dead assay” approach provides information of cell viability that relies on cell membrane integrity and functional enzymes systems, rather than subtle histologic features. However there is some controversy about reliability of “red” being “dead,” and may relate to regenerative processes that occur in vivo after thermal injury to cartilage So far, the Live/ Dead assay with confocal microscopy has been experimentally demonstrated to be reasonably accurate even though it may not describe the entire biological processes accompanying thermal injury [32]. While our study estimates the depth of tissue injury as a function of laser dosimetry, the results are only a first step in the optimization process of this procedure, and because laser injury to cartilage in vivo may trigger regenerative processes particularly within a tissue surrounded by a vibrant blood supply and a mesenchymal stem cell rich environment like perichondrium [33].

One shortcoming of the present model is that it differs from clinical LCR in that composite septal tissue is not irradiated so the effect of an outer mucosal surface was not taken into consideration. Excess composite septal cartilage grafts are difficult to obtain clinically since procedures that excise and discard full thickness septum are uncommon and at our

institution cadaveric sources are difficult to obtain within the short (i.e., <3 hours) post-mortem period needed to accomplish these type of studies. The two animal sources of septal tissue used in our lab and by others, namely, rabbit and porcine tissue differ substantially from their human counterpart in that the mucosal layer is either too thin (rabbit) or too thick (pig) to serve as a tissue model. Constructing “neo-composite” grafts by bonding mucosa of appropriate thickness obtained from heterotopic sites or xenografts to human septal remnants is an appealing approach, but the bonding process may introduce disparities in optical scattering, absorption, and anisotropy, and differences in thermal conductivity and diffusivity. These differences may limit the interpretability of any experimental data. Hence, irradiation of cartilage directly provides accurate data which would overestimate the degree of thermal damage produced during LCR. The best approach to obtain information on the extent of thermal injury might be through the use of a two or three layer thermo-optical numerical simulation [27,34]. This is beyond the scope of the current article, but is an active area of research, which we are pursuing. In clinical practice, one approach to reducing any potential damage to mucosa would be to incorporate superficial cooling measures such as those used in aesthetic laser dermatology. Regardless, laser wavelength, spot size, power and exposure time remain the dominant factors governing this laser–tissue interaction. This study characterized thermal injury as a function of laser dosimetry with the aim of identifying a range of power and exposure time pairs that do not produce full thickness injury. An infrared laser operating at 1.45 μm and short irradiation time were employed to minimize the effect of radial heat conduction and limit thermal injury to the volume of tissue encompassed with in the optical zone of light distribution. Our data suggest that for safe transmucosal irradiation of septal cartilage, the diameter of laser spot should be smaller than 3 mm to allow adjacent normal tissue to remucosalize the irradiated regions, and depth of penetration should be at least 1 mm.

Conclusions

The assay system using CLM identified the extent of non-viable chondrocytes in fresh ex vivo human septal cartilage and defined how thermal injury varies with dosimetry when using a 1.45 μm laser. This first step in the optimization process provides valuable information needed to reduce the risk of full-thickness injury during nasal LCR.

References

1. Helidonis E, Sobol E, Kavvalos G, Bizakis J, Christodoulou P, Velegrakis G, Segas J, Bagratashvili V. Laser shaping of composite cartilage grafts. Am J Otolaryngol. 1993; 14(6):410–412. [PubMed: 8285311]
2. Sobol E, Sviridov A, Omel'chenko A, Bagratashvili V, Kitai M, Harding SE, Jones N, Jumel K, Mertig M, Pompe W, Ovchinnikov Y, Shekhter A, Svistushkin V. Laser reshaping of cartilage. Biotechnol Genet Eng Rev. 2000; 17:553–578. [PubMed: 11255681]
3. Ovchinnikov Y, Sobol E, Svistushkin V, Shekhter A, Bagratashvili V, Sviridov A. Laser septochondrocorrection. Arch Facial Plast Surg. 2002; 4(3):180–185. [PubMed: 12167077]
4. Trelles MA, Mordon SR. Correction of ear malformations by laser-assisted cartilage reshaping (LACR). Lasers Surg Med. 2006; 38(7):659–662. discussion 658. [PubMed: 16799999]
5. Sviridov ASE, Jones N, Lowe J. The effect of holmium laser radiation on stress, temperature and structure of cartilage. Lasers Med Sci. 1998; 13:5.

6. Diaz SH, Nelson JS, Wong BJ. Rate process analysis of thermal damage in cartilage. Phys Med Biol. 2003; 48(1):19–129. [PubMed: 12564498]
7. Karamzadeh AM, Chang JC, Diaz S, Milner TE, Wong BJ. Long-term in vivo stability of rabbit nasal septal cartilage following laser cartilage reshaping: A pilot investigation. Lasers Surg Med. 2005; 36(2):147–154. [PubMed: 15704163]
8. Karam AM, Protsenko DE, Li C, Wright R, Liaw LH, Milner TE, Wong BJ. Long-term viability and mechanical behavior following laser cartilage reshaping. Arch Facial Plast Surg. 2006; 8(2): 105–116. [PubMed: 16549737]
9. Li C, Protsenko DE, Zemek A, Chae YS, Wong B. Analysis of Nd:YAG laser-mediated thermal damage in rabbit nasal septal cartilage. Lasers Surg Med. 2007; 39(5):451–457. [PubMed: 17565732]
10. Wong BJ, Chao KK, Kim HK, Chu EA, Dao X, Gaon M, Sun CH, Nelson JS. The porcine and lagomorph septal cartilages: Models for tissue engineering and morphologic cartilage research. Am J Rhinol. 2001; 15(2):109–116. [PubMed: 11345149]
11. Rasouli A, Sun CH, Basu R, Wong BJ. Quantitative assessment of chondrocyte viability after laser mediated reshaping: A novel application of flow cytometry. Lasers Surg Med. 2003; 32(1):3–9. [PubMed: 12516064]
12. Lu Y, Hayashi K, Hecht P, Fanton GS, Thabit G III, Cooley AJ, Edwards RB, Markel MD. The effect of monopolar radiofrequency energy on partial-thickness defects of articular cartilage. Arthroscopy. 2000; 16(5):527–536. [PubMed: 10882450]
13. Lu Y, Edwards RB III, Kalscheur VL, Nho S, Cole BJ, Markel MD. Effect of bipolar radiofrequency energy on human articular cartilage. Comparison of confocal laser microscopy and light microscopy. Arthroscopy. 2001; 17(2):117–123. [PubMed: 11172239]
14. Zuger BJ, Ott B, Mainil-Varlet P, Schaffner T, Clemence JF, Weber HP, Frenz M. Laser solder welding of articular cartilage: Tensile strength and chondrocyte viability. Lasers Surg Med. 2001; 28(5):427–434. [PubMed: 11413554]
15. Mainil-Varlet P, Monin D, Weiler C, Grogan S, Schaffner T, Zuger B, Frenz M. Quantification of laser-induced cartilage injury by confocal microscopy in an ex vivo model. J Bone Joint Surg Am. 2001; 83(4):566–571. [PubMed: 11315786]
16. Ayhan M, Deren O, Gorgu M, Erdogan B, Dursun A. Cartilage shaping with the Er:YAG laser: An in vivo experimental study. Ann Plast Surg. 2002; 49(5):527–531. [PubMed: 12439022]
17. Mordon S, Wang T, Fleurisse L, Creusy C. Laser cartilage reshaping in an in vivo rabbit model using a 154 microm Er:Glass laser. Lasers Surg Med. 2004; 34(4):315–322. [PubMed: 15083492]
18. Mordon SR, Wassmer B, Reynaud JP, Zemmouri J. Mathematical modeling of laser lipolysis. Biomed Eng Online. 2008; 7(10):10. [PubMed: 18312643]
19. Chen SS, Wright NT, Humphrey JD. Phenomenological evolution equations for heat-induced shrinkage of a collagenous tissue. IEEE Trans Biomed Eng. 1998; 45(10):1234–1240. [PubMed: 9775537]
20. Fanjul-Velez F, Arce-Diego JL. Modeling thermotherapy in vocal cords novel laser endoscopic treatment. Lasers Med Sci. 2008; 23(2):169–177. [PubMed: 17541813]
21. Dai T, Pikkula BM, Wang LV, Anvari B. Comparison of human skin opto-thermal response to near-infrared and visible laser irradiations: A theoretical investigation. Phys Med Biol. 2004; 49(21):4861–4877. [PubMed: 15584524]
22. Banerjee RK, Zhu L, Gopalakrishnan P, Kazmierczak MJ. Influence of laser parameters on selective retinal treatment using single-phase heat transfer analyses. Med Phys. 2007; 34(5):1828–1841. [PubMed: 17555264]
23. Jia W, Choi B, Franco W, Lotfi J, Majaron B, Aguilar G, Nelson JS. Treatment of cutaneous vascular lesions using multiple-intermittent cryogen spurts and two-wavelength laser pulses: Numerical and animal studies. Lasers Surg Med. 2007; 39(6):494–503. [PubMed: 17659588]
24. Jia W, Aguilar G, Verkruysse W, Franco W, Nelson JS. Improvement of port wine stain laser therapy by skin preheating prior to cryogen spray cooling: A numerical simulation. Lasers Surg Med. 2006; 38(2):155–162. [PubMed: 16493663]

25. Autrique L, Lormel C. Numerical design of experiment for sensitivity analysis—Application to skin burn injury prediction. IEEE Trans Biomed Eng. 2008; 55(4):1279–1290. [PubMed: 18390319]
26. Rossi F, Pini R, Menabuoni L. Experimental and model analysis on the temperature dynamics during diode laser welding of the cornea. J Biomed Opt. 2007; 12(1):014031. [PubMed: 17343506]
27. Chen B, Thomsen SL, Thomas RJ, Welch AJ. Modeling thermal damage in skin from 2000-nm laser irradiation. J Biomed Opt. 2006; 11(6):064028. [PubMed: 17212551]
28. Welch, Ashley J.; vG, MJC., editors. Optical-thermal response of laser-irradiated tissue. New York: Plenum Press; 1995.
29. Carslaw, HS.; Jaegar, JC., editors. Conduction of heat in solids. 2nd. London: Clarendon Press; 1959.
30. Jones N, Sviridov A, Sobol E, Omelchenko A, Lowe J. A prospective randomised study of laser reshaping of cartilage in vivo. Lasers Med Sci. 2001; 16(4):284–290. [PubMed: 11702634]
31. Jacques SL. Role of tissue optics and pulse duration on tissue effects during high-power laser irradiation. Appl Opt. 1993; 32(13):8.
32. Kaplan LD. The analysis of articular cartilage after thermal exposure: “Is red really dead?”. Arthroscopy. 2003; 19(3):310–313. [PubMed: 12627157]
33. Kaiser ML, Karam AM, Sepehr A, Wong H, Liaw LH, Vokes DE, Wong BJ. Cartilage regeneration in the rabbit nasal septum. Laryngoscope. 2006; 116(10):1730–1734. [PubMed: 17003728]
34. Zhang R, Verkruysse W, Aguilar G, Nelson JS. Comparison of diffusion approximation and Monte Carlo based finite element models for simulating thermal responses to laser irradiation in discrete vessels. Phys Med Biol. 2005; 50(17):4075–4086. [PubMed: 16177531]

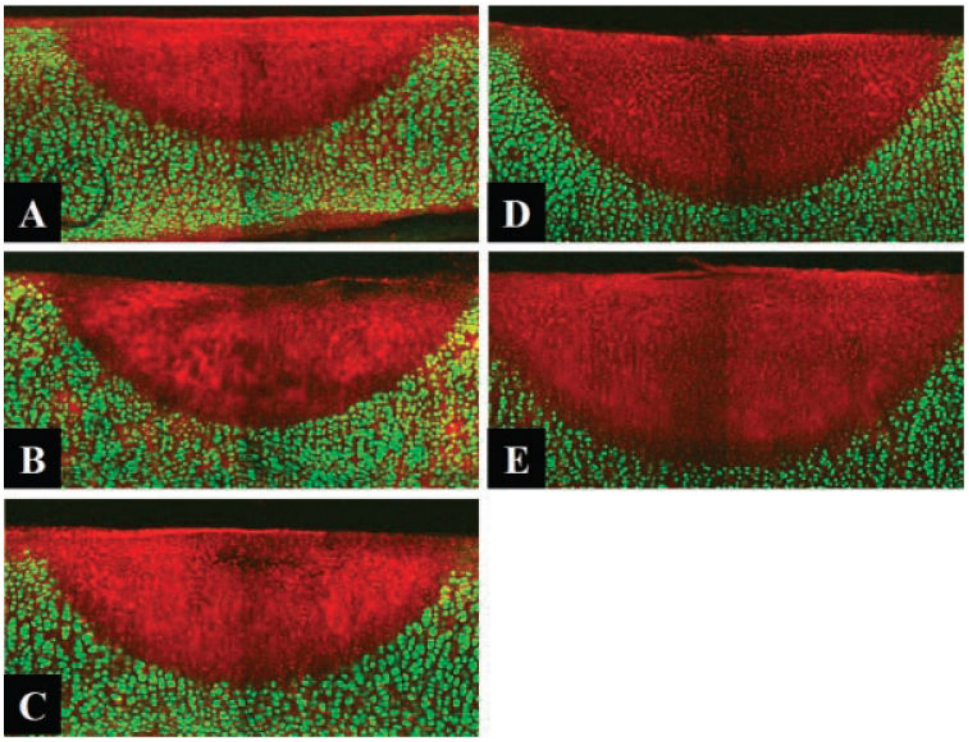

Fig. 1.

Confocal images of Live/Dead assay following 1 second. Irradiation with different power. (**A**): 1.68 W, (**B**) 2.15 W, (**C**) 2.7 W, (**D**) 3.2 W, (**E**) 3.6 W (original magnification 10×).

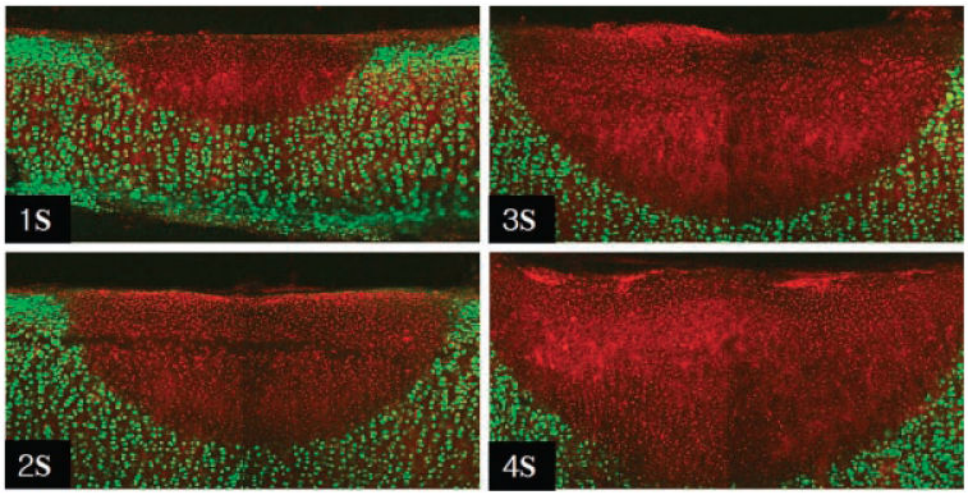

Fig. 2.

Confocal images of Live/Dead assay following 1.25 W Irradiation with different exposure time (original magnification 10×).

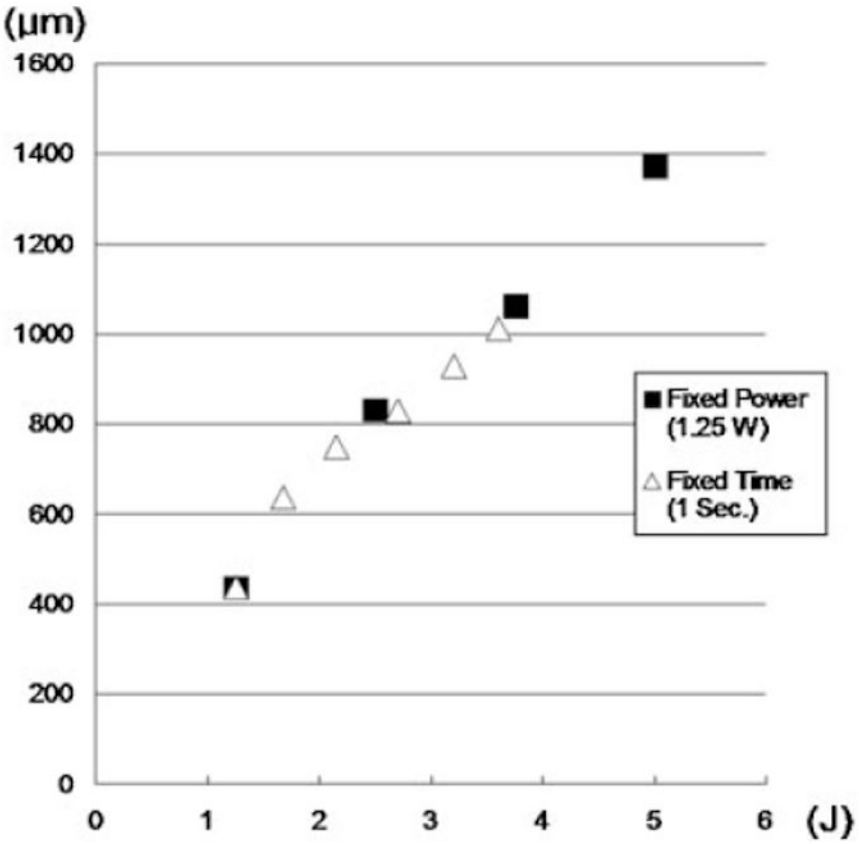

Fig. 3.
Depth of red spots as a function of total energy delivery.

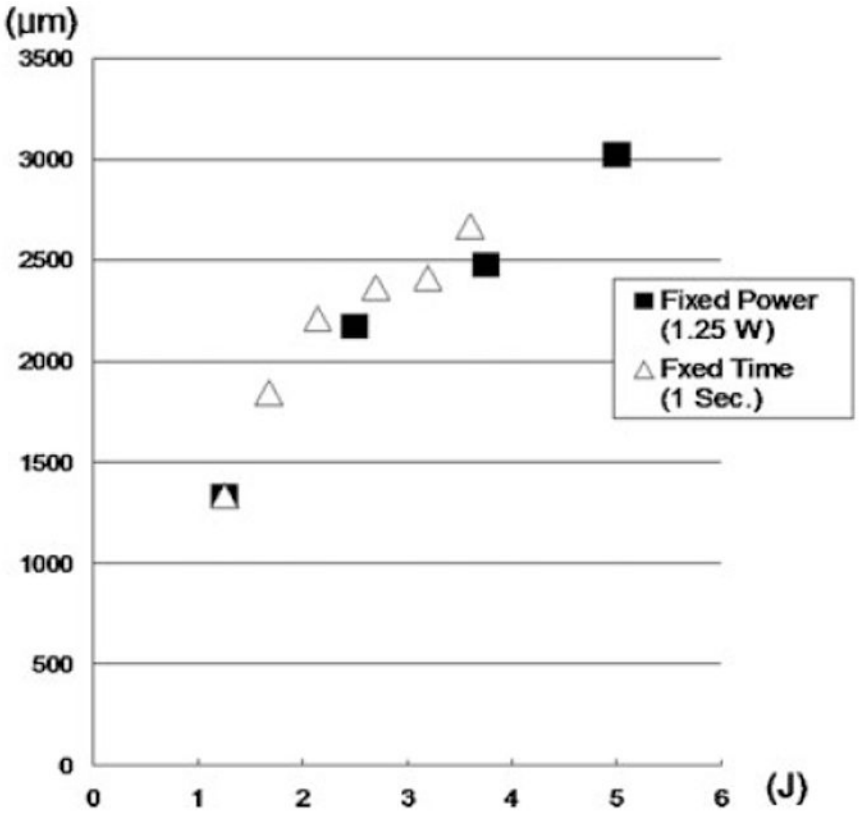

Fig. 4.
Width of red spots as a function of total energy delivery.

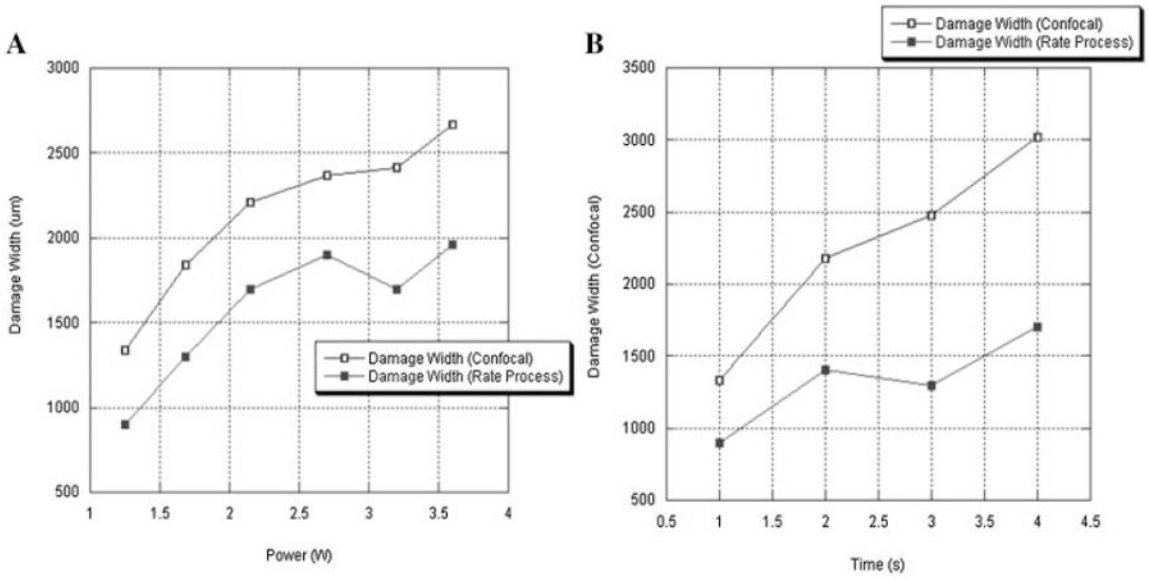

Fig. 5.

Comparison of damage width estimated using confocal image and rate process analysis. **A**: Damage width of 1 second. irradiation spots. **B**: Damage width of 1.25 W irradiation spots.

Table 1

Average (and Standard Deviation) Depth and Width of Red Spots Following 1 Second Irradiation

Power (W)	1.25	1.68	2.15	2.7	3.2	3.6
Depth (μm)	436 (± 54.7)	637 (± 22.4)	750 (± 32.7)	831 (± 18.2)	928 (± 7.5)	1,012 (± 37.1)
Width (μm)	1,336 (± 88.7)	1,843 (± 62.3)	2,210 (± 84.9)	2,366 (± 54.8)	2,411 (± 52.0)	2,666 (± 121.7)

Table 2

Average (and Standard Deviation) Depth and Width of Red Spots Following 1.25 W Irradiation

Time (second)	1[a]	2	3	4
Depth (μm)	436 (± 54.7)	839 (± 72.8)	1,061 (± 35.7)	1,372 (± 70.2)
Width (μm)	1,336 (± 88.7)	2,178 (± 111.4)	2,479 (± 53.8)	3,024 (± 160.2)

[a] Same data as Table 1.